Organic peroxides gas-particle partitioning and rapid heterogeneous decomposition on secondary organic aerosol

H. Li[1], Z. M. Chen[1], L. B. Huang[1] and D. Huang[1,*]

[1]State Key Laboratory of Environmental Simulation and Pollution Control,

College of Environmental Sciences and Engineering, Peking University, Beijing 100871, China

*Now at: School of Earth Sciences, Zhejiang University, Hangzhou, Zhejiang Province 310027, China

Correspondence to: Z.M. Chen (zmchen@pku.edu.cn)

Abstract

Organic peroxides, important species in the atmosphere, promote secondary organic aerosols (SOA) aging, affect HO_x radicals cycling, and cause adverse health effects. However, the formation, gas-particle partitioning, and evolution of organic peroxides are complicated and still unclear. In this study, we investigated in the laboratory the production and gas-particle partitioning of peroxides from the ozonolysis of α-pinene, which is one of the major biogenic volatile organic compounds in the atmosphere and an important precursor for SOA at a global scale. We have determined the molar yields of hydrogen peroxide (H_2O_2), hydromethyl hydroperoxide (HMHP), peroxyformic acid (PFA), peroxyacetic acid (PAA) and total peroxides (TPO, including unknown peroxides) and the fraction of peroxides in α-pinene/O_3 SOA. Comparing the gas-phase with the particle-phase peroxides, we find that gas-particle partitioning coefficients of PFA and PAA are 10^4 times higher than the values from theoretical prediction, indicating that organic peroxides play a more important role in the SOA formation than previously expected. Here, the partitioning coefficients of TPO were determined to be as high as $(2–3)\times10^{-4}$ m^3 μg^{-1}. Even so, more than 80% of the peroxides formed in the reaction

remain in the gas phase. Water changes the distribution of gaseous peroxides, while it does not affect the total amount of peroxides in either the gas or the particle phase. Approx. 18% of gaseous peroxides undergo rapid heterogeneous decomposition on SOA particles in the presence of water vapor, resulting in the additional production of H_2O_2. This process can partially explain the unexpectedly high H_2O_2 yields under wet conditions. Transformation of organic peroxides to H_2O_2 also preserves OH in the atmosphere, helping to improve the understanding of OH cycling.

1 Introduction

Organic peroxides are important trace components in the atmosphere, serving as reservoirs of HO_x and RO_x radicals, participating in the formation of secondary organic aerosols (SOA), and causing adverse health effects as reactive oxygen species (ROS). Recently, peroxides are found to play a key role in the aging of SOA. The particle-bound organic peroxides undergo atmospheric photolysis with a lifetime of about 6 days (Epstein et al., 2014), and decline significantly within the mean SOA age of 4–7 days (Rudich et al., 2007). A laboratory experiment on the photolysis of SOA shows a high yield of hydroxyl radicals (OH), which are considered to form from the decomposition of peroxides (Badali et al., 2015). This OH may cause the in-particle oxidation of SOA.

Model studies have tried to simulate the SOA formation in chamber experiments, but great discrepancies still exist between predicted and observed results (Camredon et al., 2010; Hoffmann et al., 1997; Griffin et al., 1999; Cocker III et al., 2001; Saathoff et al., 2009; Presto et al., 2005; Pye and Seinfeld, 2010; Farina et al., 2010). Jenkin (2004) added the formation of dimers and improved the simulation, especially at the beginning of SOA formation. Organic peroxides were found to be highly abundant in SOA (Ziemann, 2005; Docherty et al., 2005; Surratt et al., 2006; Nguyen et al., 2010; Bateman et al., 2011; Mertes et al., 2012; Epstein et al., 2014), possibly in the form of oligomers, which are even more important than carboxylic acids (Bonn et al., 2004). In order to improve the simulation of the production of the SOA mass within the chamber, explicit parameters about gas-particle partitioning of organic peroxides are urgently needed.

The reactions and processes that generate or remove peroxides have been studied for many years. Cross-reactions of organic peroxy radicals (RO_2) and the hydroperoxy radical (HO_2) and

self-reactions of HO_2 are thought to be major sources of organic peroxides and hydrogen peroxide (H_2O_2), respectively, in the atmosphere. Ozonolysis of biogenic volatile organic compounds (VOC) also produces H_2O_2 in high yields although its mechanism is unknown (Zhang et al., 2009; Huang et al., 2013). Hydrolysis and reaction with OH are the main removal pathways for both organic peroxides and H_2O_2, and dry/wet deposition removes only a small portion of peroxides (Khan et al., 2015). However, existing theories about sources of and removal of peroxides cannot account for the field observation results. Model simulations showed an overestimation on total peroxides (TPO) and a underestimation on H_2O_2 as compared with field records in the airborne GABRIEL (Guyanas Atmosphere-Biosphere exchange and Radicals Intensive Experiment with the Learjet) field campaign (Kubistin et al., 2010), indicating the existence of possible underestimated or new removal paths for organic peroxides and overestimated or new formation paths for H_2O_2. Field observations and laboratory experiments showed that particulate components, possibly particle-bound organic peroxides, could be transformed to H_2O_2. Arellanes et al. (2006) found that H_2O_2 in ambient SOA solution was 200–1000 times greater than expected levels based on the gas-liquid partitioning, implying that almost all H_2O_2 is generated from SOA solution. Wang et al. (2011) investigated several kinds of SOA derived from the oxidation of α-pinene, β-pinene, and toluene, and came to the similar conclusion that more than 97.5% H_2O_2 arose from SOA formation rather than from gas-liquid partitioning. However, this process happens in SOA solution and the amount of H_2O_2 produced by such a pathway is too small to account for the large discrepancy between observations and simulations for the gas-phase H_2O_2.

The effect of water on peroxides is complex. Laboratory experiments suggested that yields of particle-phase total peroxides in the ozonolysis of alkenes are not influenced by water vapor (Docherty et al., 2005). Unlike the total peroxides, yields of individual peroxides depend on relative humidity (RH). Yield of H_2O_2 increases under wet conditions (Becker et al., 1990; Hewitt and Kok, 1991; Simonaitis et al., 1991; Gäb et al., 1995; Huang et al., 2013), while the yields of bis-hydroxymethyl hydroperoxide and three unknown organic peroxides decrease under wet conditions (Huang et al., 2013). Theoretical studies suggest that water helps both the formation and decomposition of organic peroxides. Water can react with stabilized Criegee Intermediates (SCIs) and generate hydroxyalkyl hydroperoxides (HAHPs). It has been proposed that not only isolated water molecules, but also water dimers react with SCI, and the

latter path could even be more important (Ryzhkov and Ariya, 2004). Numerous laboratory experiments support this proposal (Chao et al., 2015; Lewis et al., 2015; Berndt et al., 2014). As a result, the reaction with water dimers will be the largest sink for CH_2OO. However, the quantum-chemical calculations predict that the larger SCIs react more slowly with water, both the water monomer and dimer (Vereecken et al., 2014). Water also helps gas-phase decomposition of HAHPs, although the decomposition rate constant is small according to the theoretical calculations (Crehuet et al., 2001; Aplincourt and Anglada, 2003).

This study investigates the ozonolysis of α-pinene, which is considered as one of the largest contributors to SOA and a dominant source of organic peroxides on a global scale (Khan et al., 2015), focusing on the formation of peroxides in both the gas and the particle phase. Gas-particle partitioning and water effect are examined carefully.

2 Material and methods

2.1 Chemicals

α-Pinene (Aldrich, 99%), cyclohexane (Sigma-Aldrich, ≥ 99.7%), potassium iodide (Alfa Aesar, 99.9%), hydrogen peroxide (Alfa Aesar, 35 wt %), *ortho*-phosphoric acid (Fluka, 85–90%), hemin (Sigma, ≥ 98.0%), 4-hydroxyphenylacetic acid (Alfa Aesar, 99%), ammonia solution ($NH_3 \cdot H_2O$, Beijing Tongguang Fine Chemicals Company, 25.0–28.0%), ammonium chloride (NH_4Cl, Beijing Chemical Works, ≥ 99.5%), ultrapure water (18 MΩ, Millipore), N_2 (≥ 99.999%, Beijing Haikeyuanchang Practical Gas Company Limited, Beijing, China), O_2 (≥ 99.999%, Beijing Haikeyuanchang Practical Gas Company Limited, Beijing, China), and polytetrafluoroethylene (PTFE) filter membrane (Whatman Inc., 47 mm in diameter) were used in this study.

2.2 Apparatus and procedures

A flow tube reactor (2 m length, 70 mm inner diameter, quartz wall) equipped with a water jacket for controlling temperature was used to investigate the ozonolysis of α-pinene. All the

experiments were conducted at 298±0.5 K and in dark. O_3 was generated by the photolysis of O_2 in a 2 L quartz tube with low-pressure Hg lamp, and the detailed quantification method of O_3 was described in our previous study (Chen et al., 2008). O_3 (~25 ppmv) was used in the experiments. α-Pinene gas was generated by passing a flow of N_2 over liquid α-pinene in a diffusion tube at the selected controlled temperature. The initial concentration of α-pinene, determined by gas-chromatography-flame ionization detector (GC-FID, Agilent 7890A, USA), was ~273 ppbv in the experiments. Water vapor was generated by passing N_2 through a water bubbler. The mixing gases, including α-pinene, O_3, and dry or wet synthetic air (80% N_2 and 20% O_2), were continuously introduced into the reactor with a total flow rate of 4 standard L min^{-1} (standard liters per minute) and a residence time of 120 s. The relative humidity (RH) was controlled at two levels: <0.5% RH (dry conditions) and 60% RH (wet conditions). Gas from the reactor (2 standard L min^{-1}) was directed into a coil collector and scrubbed by H_3PO_4 stripping solution (5×10^{-3} M, pH 3.5) for hydroperoxides analysis. SOA produced from the ozonolysis of α-pinene were collected onto a PTFE filter for 4 h at a flow rate of 4 standard L min^{-1}, and the mass of SOA on the filter was immediately measured by a semi-micro balance (Sartorius, Germany). After that, each loaded filter was extracted with 20 mL H_3PO_4 solution (5×10^{-3} M, pH 3.5) using a shaker (Shanghai Zhicheng ZWY 103D, China) at 180 rpm and 4 °C for 15 min, and then the SOA solution was immediately analyzed to determine the particle-phase peroxides. Each SOA solution was analyzed 7 times at different times to investigate the evolution of SOA solution.

To explore the effect of water vapor on the formation of peroxides in the ozonolysis, two-stage reaction experiments were designed and carried out. In the first stage, dry synthetic air (2 standard L min^{-1}) with α-pinene (~275 ppbv) and O_3 (~42 ppmv) entered the first 2 L flow-tube reactor; in the second stage, the gas passed through the second 2 L flow-tube reactor but with the addition of dry or wet synthetic air (2 standard L min^{-1}). The residence time was 68 s in the first reactor and 34 s in the second reactor. The concentration of α-pinene at the outlet of the first reactor was found to be below the GC-FID detection limit (< 5 ppbv), meaning that α-pinene was almost completely consumed before the gas entered the second reactor. Thus, water vapor appearing in the second reactor only affected the products from the first reactor. A filter was placed at the outlet of the first reactor or second reactor to collect SOA when necessary.

2.3 Peroxides analysis

The low-weight molecular peroxides were measured using high-performance liquid chromatography (HPLC, Agilent 1100, USA) coupled with a post-column derivatization module and fluorescence detection, and the concentration of total peroxides was determined by an iodometric spectrophotometer method. Details about the HPLC-fluorescence method have been reported in our previous study (Hua et al., 2008). Briefly, this method is based on the reaction of *p*-hydroxyphenylacetic acid (POPHA) with organic hydroperoxides or hydrogen peroxide in the catalysis of the hemin forming POPHA dimer (2,2′-bisphenol-5,5′-diacetic acid), which is a fluorescent substance, and then is quantified by fluorescence detector. The separation of peroxides was implemented by column chromatography before the peroxides were reacted with POPHA. The synthetic method for organic peroxides standards is described in our previous study (Huang et al., 2013).

The iodometric spectrophotometric method is used to quantify all classes of peroxides (ROOR′, ROOH and H_2O_2), with the exception of tertiary dialkyl peroxides, in the aqueous phase without distinction (Banerjee and Budke, 1964). Peroxyhemiacetals formed in α-pinene ozonolysis can be measured with this method. Excess potassium iodide reacts with peroxides producing I_3^- ion (R1), which can be quantified by UV/VIS spectrophotometry.

$$3I^- + H_2O_2 + 2H^+ \rightarrow I_3^- + 2H_2O \quad \text{(R1)}$$

α-Pinene SOA is freely soluble in polar solvents, e.g., water, acetonitrile and methanol, but it is poorly soluble in nonpolar solvents, e.g., chloroform and toluene (Nguyen et al., 2010). Hence, a H_3PO_4 solution, as a kind of polar solvent, could entirely extract SOA from filters. The HPLC fluorescence method uses H_3PO_4 solution as a solvent for peroxides such as H_2O_2, hydromethyl hydroperoxide (HMHP), performic acid (PFA), and peracetic acid (PAA) which are more stable in acidic solution than in pure water (Zhou and Lee, 1992). In order to be comparable with the HPLC fluorescence method, SOA loaded filters were also extracted by H_3PO_4 solution. The influence of pH on extraction efficiency is discussed in the Supplement. In this study, SOA solution (2.5 mL) was added into a 10 mL airtight micro reaction vessel (Supelco, USA). Each solution was then purged of oxygen by bubbling with N_2 for 5 min. After purging, an aqueous solution of KI (250 μL, 0.75 M) was added into the vessel. The vessel was then capped tightly, covered with aluminium foil, and allowed to stand in the dark for 12–24 h.

The solution absorbance was then measured at 420 nm by an UV/VIS spectrophotometer (SHIMADZU UV-1800, Japan). The efficiency of peroxide measurements was discussed in the supplement.

3 Results and discussion

3.1 Gas-particle partitioning of peroxides

3.1.1 Particle-phase peroxides

We measured the different mass values of SOA produced from the ozonolysis of α-pinene at different RHs in the presence or absence of the OH scavenger cyclohexane, and found that the typical in-reactor SOA concentration was 450–650 μg m^{-3}. A comparison of the aerosol mass yields (Y_{SOA}), defined as the ratio of the formed aerosol mass to the consumed α-pinene mass, (Table 1) indicated that while the SOA yields were independent on the presence of water vapor, they decreased in the presence of OH scavenger.

Organic peroxides are considered to be one of the major constituents in SOA (Docherty et al., 2005; Ziemann, 2005; Surratt et al., 2006; Nguyen et al., 2010; Mertes et al., 2012; Kidd et al., 2014; Badali et al., 2015) (Table S1). The sensitivity of the iodometric method to ROOR is critical to obtain an accurate concentration of total peroxides since peroxyhemiacetals are a significant component (Docherty et al., 2005). In the present study, we determined the total molar concentration of peroxides in SOA using the iodometric method. Stability of peroxides in SOA stored on-filter was also tested, and the results show that peroxides concentration decrease with increasing sitting time (Figure S4). Hence, the peroxides in SOA were determined immediately after collection. Here, the mass fraction of peroxides in SOA ($F_{peroxides}$) is defined as the ratio of mass of particle-bound peroxides to SOA mass, which is defined as follows:

$$F_{peroxides} = \frac{m_{peroxides}}{m_{SOA}} \quad (1)$$

where $m_{peroxides}$ is the mass of particle-bound peroxides, such as PFA, PAA and TPO, and m_{SOA} is the mass of SOA. Assuming that the average molecular weight of peroxides is 300, we obtained the mass fraction of total peroxides in SOA (F_{TPO}) as ~0.21 (Table 1), which is

consistent with 0.22 reported by Epstein et al. (2014), but less than 0.47 reported by Docherty et al. (2005) and 0.34 reported by Mertes et al. (2012). Several factors, such as the presence of OH scavengers, reactor type, extraction method, SOA mass measurements, and SOA density assumptions, may cause these discrepancies. In addition to the concentration of total peroxides, we measured the concentration of two small organic peroxides peroxyformic acid (PFA) and peroxyacetic acid (PAA) in SOA and calculated the contribution of PFA (F_{PFA}) and PAA (F_{PAA}) to SOA mass (Table 1). Under dry conditions, the F_{PFA} and F_{PAA} were 0.35 ±0.06 and 0.11 ±0.04 ng μg^{-1}, respectively, without the OH scavengers and 0.14 ±0.00 and 0.09 ±0.01 ng μg^{-1}, respectively, with cyclohexane. After adding water vapor, F_{PFA} did not significantly change, but F_{PAA} approached 0.

3.1.2 Gas-phase peroxides

In addition to the particle phase peroxides, we measured the gas-phase peroxides generated in the ozonolysis of α-pinene. Here, the molar yield of gaseous peroxides ($Y_{peroxides}$) is defined in eq (2):

$$Y_{peroxides} = \frac{\Delta peroxides}{\Delta \alpha\text{-pinene}} \quad (2)$$

where Δperoxides are moles of formed gaseous peroxides, such as HMHP, PFA, PAA and TPO, and Δα-pinene are moles of consumed α-pinene. The molar yield of total peroxides (Y_{TPO}) were estimated to be nearly the same under both dry conditions and wet conditions in the absence of OH scavengers (Table 1), indicating that total yield of peroxides was unaffected by water vapor. Moreover, when we employed the MCM v3.1 mechanism to simulate the present reaction system, the modelled yield of total peroxides was about 0.25, consistent with our experimental result. The model results also suggested that hydroperoxides account for more than 99% of total peroxides. The yields of HMHP (Y_{HMHP}), PFA (Y_{PFA}) and PAA (Y_{PAA}) are shown in Table 1. Compared with dry conditions, Y_{HMHP} and Y_{PFA} doubled under wet conditions, while Y_{PAA} increased only slightly. However, yields of these three organic peroxides were all lower in the presence of OH scavengers, indicating the importance of OH in the formation of small organic peroxides.

Considering that all the peroxides originally existed in the gas phase at the beginning of the ozonolysis of α-pinene, we estimated the fraction of peroxides that entered the particulate phase from the gas phase through gas-particle partition based on measured peroxides in the particle and gas phases. The fraction of particulate TPO in gaseous and particulate TPO (TPO(p)/TPO(g+p)) were essentially the same (Table 1) under both wet and dry conditions. To the best of our knowledge, for the ozonolysis of α-pinene, this is the first report of the yield of gas-phase total peroxides (including hydrogen peroxide and organic peroxides) and the gas-particle partitioning fraction.

The gas-particle partitioning coefficient (K_p) describes the partitioning ability of a given species, calculated as follows (Odum et al., 1996):

$$K_p = \frac{C_a}{C_g C_{om}} \quad (3)$$

where C_a is the concentration of this species in the aerosol phase, μg m^{-3}; C_g is the concentration of this species in the gas phase, μg m^{-3}; and C_{om} is the total concentration of condensed organic matter, μg m^{-3}. Based on the gas-phase peroxides concentration, particle-phase peroxides concentration, and the aerosol yields summarized in Table 1, we can obtain the observed K_p (Table 2).

The Pankow absorption model (Pankow, 1994) is the most widely accepted mechanism to explain the gas-particle partitioning, and has been used to predict aerosol yields in chamber experiments (Cocker III et al., 2001; Jenkin, 2004; Yu et al., 1999). Theoretical K_p can be calculated by the following equation:

$$K_p = \frac{7.501 \times 10^{-9} RT}{MW_{om} \varsigma p_L^{\circ}} \quad (4)$$

where R is the ideal gas constant, J K^{-1} mol^{-1}; T is the temperature, K; MW_{om} is the mean molecular weight of the condensed organic material, g mol^{-1}. In the present study, MW_{om} is estimated to be 130 g mol^{-1}; ς is the activity coefficient of the given species in the condensed organic phase, and here, is assumed to be unity; p_L° is the liquid vapour pressure of this species, Torr. The theoretical p_L° can be calculated by an expended, semi-empirical form of Clausius-

Clapeyron equation (Baum, 1997). Theoretical gas-particle partitioning coefficients of PFA and PAA are shown in Table 2.

The observed gas-particle partitioning coefficients of PFA, PAA and TPO were $(3–9)\times10^{-5}$, $(2–4)\times10^{-5}$ and $(2–3)\times10^{-4}$ m^3 μg^{-1}, respectively (Table 2), which, to the best of our knowledge, are reported here for the first time. However, the long time collection for SOA do have effects on gas- and particle-phase constituents possibly due to re-partitioning of species between the two phases. Collected SOA mass and peroxides amount per unit time decreases slightly with increasing collection time, and peroxides amount decreases faster than SOA mass (Supplement). Hence, the gas-particle partitioning coefficients of peroxides given here are underestimated by about 21%. Compared with the observed K_p values, theoretical K_p values of PFA and PAA, 2×10^{-9} m^3 μg^{-1} and 4×10^{-9} m^3 μg^{-1}, respectively, were lower by a factor of 10^4. This large difference between observed and theoretical K_p values has also been reported previously (Cocker III et al., 2001; Jenkin, 2004; Kamens and Jaoui, 2001). Jenkin (2004) considered the existence of a significant systematic error, which is independent of key parameters involved in prediction of K_p values, or the inability to interpret the Pankow absorption model. After inducing a species-independent scaling factor of ca. 120 for all partitioning species, Jenkin obtained a reasonable simulation of the final experimental aerosol concentration, but was still unable to interpret the early stages of aerosol accumulation. In addition to the absorptive partitioning mechanism, the participation of bi- and multifunctional acid dimers in the aerosol formation process was also considered, resulting in the presentation of simulated results. Organic peroxides are also important compounds in dimer formation, for instance, hydroperoxides can react with aldehydes subsequently producing peroxyhemiacetals (Tobias and Ziemann, 2000; Tobias and Ziemann, 2001; Ziemann, 2005). The vapor pressures of hydroperoxides decreased in the formation of peroxyhemiacetal by an additional factor of ~10^2–10^5 (Tobias and Ziemann, 2000), which could partially explain the large discrepancy between the observed and theoretical gas-particle partitioning coefficient. However, related thermodynamic and kinetic parameters need further study to resolve the problem.

3.2 Evolution of SOA in the aqueous phase

We investigated the evolution of SOA in the aqueous phase, focusing on the change of H_2O_2 in SOA. The initial concentration of H_2O_2 was low, but it increased rapidly in the first 3.5 h,

approaching the peak at ~7.5 h, and then decreased slowly, meaning the existence of a sustained release of H_2O_2 in the SOA solution at room temperature (298 K) (Figure 1). The molar fraction of peak-H_2O_2 to total peroxides in SOA (H_2O_2(p)/TPO(p)) under dry conditions was twice as high as that observed under wet conditions in the absence of OH scavengers (Table 1). The contribution of H_2O_2 to the SOA mass (F_{H2O2}) was 1.9 times higher under dry conditions (5.09 ± 0.99 ng μg^{-1}) than under wet conditions (2.67 ± 0.17 ng μg^{-1}) (Table 1). In the presence of cyclohexane, H_2O_2(p)/TPO(p) was slightly higher under dry conditions than wet conditions (0.09 ± 0.00 and 0.06 ± 0.00, respectively) while F_{H2O2} values were not significantly affected by RH (Table 1). Our observations consist with those of Wang et al. (2011) who studied α-pinene-derived SOA, and measured the F_{H2O2} as 2.01 ± 0.76 ng μg^{-1}, which was unchanged by a variety of oxidants (NO/light, O_3 and O_3/cyclohexane) over the range of 14–43% RH.

The sustained release of H_2O_2 coupled with the attenuation of total peroxides provided experimental evidence for the hypothesis that the decomposition/hydrolysis of organic peroxides generates H_2O_2. The decay of H_2O_2 in SOA solution after 18 h is a comprehensive phenomenon including formation and decomposition, and the rate was estimated to be 0.06 μM h^{-1} and 0.03 μM h^{-1} for SOA produced under dry and wet conditions, respectively. To assess the formation, we determined the decomposition rates of pure H_2O_2 at different concentrations. When the H_2O_2 concentration was ~5 μM (~2.5 μM), the rate of decomposition was 0.11 μM h^{-1} (0.05 μM h^{-1}). The H_2O_2 concentrations were equivalent with those of H_2O_2 in SOA solution. Thus, we can estimate H_2O_2 formation in the SOA solution after 18 h to have a rate of 0.05 μM h^{-1} under dry conditions and 0.02 μM h^{-1} under wet conditions. As shown in Figure 2, the peroxycarboxylic acids (PCAs) (PFA and PAA), decayed quickly while the HAHP (HMHP) decayed slowly. Hence, the formation of H_2O_2 after 18 h could be attributed to the decomposition of HAHPs. However, in the first 7.5 h period, H_2O_2 increased rapidly which is more consistent with the decay of PCAs rather than HAHPs. Not all the organic peroxides decayed during the observation time, since the attenuation of TPO almost stopped after 40 h. The residual peroxides were more stable, possibly due to the formation of ROOR by oligomerization.

3.3 Unexpectedly high levels of H_2O_2 in the gas phase

Table 1 shows the molar yields of gas-phase H_2O_2. The H_2O_2 yield in the absence and presence of cyclohexane was essentially the same in dry conditions, but under conditions of high RH increased to 0.16 ±0.01 in control studies and to 0.14 ±0.02 in the presence of cyclohexane. Thus, the presence of water vapor elevated the H_2O_2 yield, while the presence of a radical scavenger had no effect. Previous studies on gas-phase H_2O_2 yields of the ozonolysis of α-pinene are reviewed (Table S2). Becker et al. (1990) firstly reported that the presence of water vapor will significantly promote the H_2O_2 yield, and our work confirmed this observation. However, our measured values of H_2O_2 were ten times higher than those reported by others under both dry and wet conditions, except that by Simonaitis et al. (1991). Differences in reactant concentration, reactor type and measuring methods account for these discrepancies. Worth noting, the reactants concentrations used in these previous and our experiments are very high, therefore, yields of peroxides may not represent actual yields of peroxides in oxidation of α-pinene in nature (Supplement).

The source of gas-phase H_2O_2 remains unclear. We suggest that further ozonolysis and OH oxidation of gaseous products and reactants in the aqueous phase during and after gas collection are not likely to be the main sources of H_2O_2. In this study, the online GC-FID test showed that α-pinene was completely consumed in the gas phase. Hence, the contribution of aqueous-phase α-pinene ozonolysis to the measured H_2O_2 in the coil collector should be negligible. The main gas-phase non-peroxy organic products of α-pinene ozonolysis are carbonyls and organic acids, e.g., pinonaldehyde, formaldehyde, acetone and pinic acid; these compounds without carbon-carbon double bonds cannot be oxidized by O_3. The ozonolysis of α-pinene produces the OH radical in high yield (0.68–0.91) (Berndt et al., 2003), which potentially oxidizes carbonyls and organics. However, we observed no difference of Y_{H2O2} in the absence and presence of OH scavengers, indicating that OH oxidation in the aqueous phase may not be a source of H_2O_2.

Decomposition/hydrolysis of organic peroxides in the aqueous phase during and after gas collection are also found to be a minor source of gas-phase H_2O_2. HAHPs and PCAs, two kinds of organic peroxides, are the probable candidate for generating H_2O_2. HAHPs are the main products of the reaction of SCI with water molecules and dimers (Ryzhkov and Ariya, 2004), and they can decompose to H_2O_2 plus the corresponding aldehyde or H_2O plus the

corresponding organic acid (Hellpointner and Gäb, 1989). The hydrolysis of PCAs, which are generated from the reaction of RC(O)OO with HO_2, is another possible source of H_2O_2. Several kinds of PCAs have been qualitatively observed in the ozonolysis of α-pinene (Venkatachari and Hopke, 2008). In this study, we quantitatively observed PFA and PAA in the gas phase (Table 1), and simulated the formation of PCAs using MCM v3.1 mechanism. Model results showed that the yield of total PCAs was extremely low, 0.0005, and PAA contributed more than half of the yield while the formation pathway of PFA was not included. The large discrepancy between modelled and experimental results indicates that PCAs play a more important role than was expected previously. We estimate the H_2O_2 generated from organic peroxides in the aqueous phase by measuring the decomposition/hydrolysis rate of organic peroxides. Considering the effects of concentration, coexisting components, and ionic strength, we conducted the measurements with coil collection solutions rather than with synthesized samples. The decomposition/hydrolysis of organic peroxides is a pseudo-first order reaction due to the excess of the other reactant, i.e., water. The decay rate constants of HMHP, PFA and PAA were determined to be 0.09, 1.06 and 0.64 h^{-1}, respectively (Figure 2). Larger HAHPs were less active compared with HMHP and should have lower decay rate constants. If all the TPO are composed of HAHPs and the production of H_2O_2 plus aldehydes is the only decomposition pathway of HAHPs, the upper bound of H_2O_2 formed in the aqueous phase within 8 min may be estimated to be 1.2% of TPO. However, the observed ratio of gas-phase H_2O_2 to TPO was 28%–78%, indicating that the aqueous-phase decomposition of HAHPs is insignificant. Compared with HMHP, the decay rates of PFA and PAA were quite high. Assuming that all the TPO, except for PFA, are PCAs and their decay rates were the same as PAA's, H_2O_2 formed in aqueous phase within 8 min is estimated to be 13.2% of TPO, which can partially explain the observed H_2O_2 level. However, the yield of PCAs in the ozonolysis of α-pinene is predicted to be low in the MCM v3.1 model. The experimental results mentioned above concluded that the aqueous-phase formation of H_2O_2 is not important, for the decay rate of HAHPs was too slow, and the amount of PCAs was too low although their decay rate was higher.

Whether the self-reaction of HO_2 and decomposition of HAHP in the gas phase are the main sources of H_2O_2 is discussed here. The self-reaction of HO_2 is considered to be the main source of ambient H_2O_2 (Lee et al., 2000; Reeves and Penkett, 2003) and occurs in the ozonolysis of

α-pinene. When we estimated the contribution of this pathway to the observed H_2O_2 from α-pinene ozonolysis using MCM v3.1 mechanisms, the yield was less than 0.001 under both dry and wet conditions, meaning that this pathway is negligible. Chamber experiments showed that SCI mainly reacts with water vapor even under dry conditions (Jenkin, 2004), and the major product is HAHP. Aplincourt and Anglada (2003) considered that the unimolecular decomposition of gaseous HAHPs was unlikely to occur, and only the water-assisted decomposition was efficient in the gas phase. They estimated the water-assisted decomposition rate constant of 2-propenyl α-hydroxy hydroperoxide to be 1.5×10^{-30} cm^3 $molecule^{-1}$ s^{-1} by quantum chemical calculation. Based on their work, the gas-phase decomposition fraction of HAHP in 2 min can be calculated to be less than 0.01%, which is too small to account for the H_2O_2 observed in our experiments.

In summary, the high H_2O_2 yields in the gas phase cannot be explained by the bias caused by measuring method and the current formation mechanism of H_2O_2. There may exist an unknown or underestimated pathway producing H_2O_2. In section 3.4, we propose that gaseous organic peroxides can undergo rapid heterogeneous decomposition in the presence of water and producing H_2O_2.

3.4 Rapid heterogeneous decomposition of gaseous organic peroxides

Our results demonstrate that water vapor has no significant effect on either the yield of total peroxides (combining gaseous and particulate peroxides) or the contribution of peroxides to SOA mass. However, water vapor does change the concentrations of H_2O_2, PFA and PAA in the gas phase and particle phase in an opposite manner (Table 1). In the presence of water vapor, H_2O_2 yield increased dramatically by ~300%, and gas-phase H_2O_2/TPO increased from 0.26 to 0.78. Yields of HMHP, PFA and PAA also increased with the presence of water vapor. These results clearly indicate that water vapor can change the formation and distribution of peroxides.

We carried out a series of two-stage experiments using two reactors under various scenarios to further study the effect of water vapor on peroxides (Table 3). In scenario 1d, no water vapor was added and a filter was used to intercept SOA entering the coil collector, which is similar to measuring H_2O_2 under dry conditions with one reactor. The concentration of H_2O_2 observed in the coil collection solution under this condition was considered to be the baseline value, 100%.

When the filter was placed at the outlet of the first reactor (scenario 2d) instead of at the second reactor, the concentration of H_2O_2 was 103 ±6%, almost the same as the baseline, indicating that the coexistence of gaseous products and SOA will not lead to the formation of H_2O_2. In scenario 2w, a filter was placed at the outlet of the first reactor and water vapor was added to the second reactor, resulting in the coexistence of gaseous products and water vapor (50% RH) in the second reactor. The concentration of H_2O_2 observed in this scenario was 87%, slightly lower than the baseline, possibly due to losses on the wall of the reactor under wet conditions, which has been reported to be 5% for H_2O_2 at 50% RH (Huang et al., 2013). When we maintained the water vapor and moved the filter to the outlet of the second reactor (scenario 1w), the H_2O_2 concentration increased to 165 ±6% of baseline. In scenario 3w, with water vapor added to the second reactor and without a filter in the gas flow, the H_2O_2 concentration was 172 ±5%, almost the same as that in scenario 1w. In scenario 3d, no water vapour and no filter were used, but a high H_2O_2 concentration, 164 ±9%, was also observed. For scenarios 1w, 3w, and 3d, where H_2O_2 increased by ~67%, gaseous products, SOA, and water were all present in the second reactor or coil collector. The coexistence of gaseous products and water vapor (see scenario 2d and 2w), the coexistence of gaseous products and SOA (see scenario 1d and 2d), and the coexistence of SOA and water (see section 3.3) did not result in a high yield of H_2O_2. We therefore concluded that the presence of three components together, the gaseous products, SOA, and water, was necessary for a high yield of H_2O_2. Once the gaseous products and SOA had been in contact with water vapor in the second reactor, the levels of H_2O_2 were increased to the same extent, whether or not these compounds were mixed with condensed water (see scenario 1w and 3w), indicating that the process producing H_2O_2 in the gas phase is quite rapid.

When we measured the total peroxides formed from gaseous products and SOA in scenarios 1d and 1w, the results showed that for these two scenarios, the levels of the total peroxides in both gaseous products and SOA were not significantly different, indicating that SOA does not change in the presence of water vapor and no new peroxides formed in the gas phase. This outcome supports the idea that the increment of H_2O_2 comes from the redistribution of gaseous peroxides, which is induced by the heterogeneous decomposition of gaseous products in the presence of both SOA and water. Based on the measured increment of H_2O_2 and concentration of gaseous total peroxides, we concluded that 18% of the gaseous total peroxides undergo rapid heterogeneous decomposition.

Heterogeneous reactions of trace gases on the surface of particles relevant to the atmosphere have been studied for many years. The investigated trace gases, including nitrogen oxides (e.g., HNO_3, NO_2 and N_2O_5), SO_2, O_3, H_2O_2 and oxygenated VOCs (Liggio et al., 2005; Kroll et al., 2005; Prince et al., 2007; Zhao et al., 2010; Zhao et al., 2011; Zhao et al., 2014; Huang et al., 2015), could react with the active sites on the surfaces of mineral dust (Goodman et al., 2001; Fu et al., 2007). Unlike mineral dust, however, SOA has no such active sites. The elucidation of the mechanism of the rapid heterogeneous decomposition of organic peroxides on SOA particles remains a great challenge and needs urgent study.

4 Conclusions and atmospheric implications

Our laboratory study has provided more evidence that organic peroxides are important components of SOA derived from the ozonolysis of alkenes. In the case of α-pinene, organic peroxides account for ~21% of the SOA mass and this fraction is not affected by RH and the presence of OH scavengers. More interestingly, the gas-particle partitioning coefficients of organic peroxides have been estimated for the first time based on the measurements of both gaseous and particulate peroxides. Due to the long-time collection for SOA, these coefficients reported here are lower bounds in this study. For PFA and PAA, the observed values were 10^4 times higher than that of the theoretical value calculated by the Pankow absorption model. This discrepancy indicates a more important role of peroxides in SOA formation than expected previously and the existence of yet undefined mechanisms in addition to the absorption. The reaction of organic hydroperoxides with carbonyls forming peroxyhemiacetals may explain part of the enhancement of the partitioning of peroxides. However, the kinetic parameters of peroxyhemiacetal formation are lacking. The explicit mechanisms of gas-particle partitioning and the determination of gas-particle partitioning coefficients of larger organic peroxides deserve further study to improve the simulation of SOA mass.

We also examined gas-phase peroxides. The yield of gaseous total peroxides was ~0.22, which was independent of RH and OH scavengers. The MCM v3.1 mechanism predicted this yield but failed to explain the yields of individual peroxides, i.e., H_2O_2, HMHP, PFA and PAA, indicating that our previous understanding of α-pinene ozonolysis was insufficient. For H_2O_2 with a yield of 0.048 under dry conditions and 0.16 under wet conditions, the known pathways, including dissolution of SOA, aqueous oxidation of gaseous compounds, and

460 decomposition/hydrolysis of organic peroxides in the aqueous phase, cannot explain such an
461 unexpectedly high yield of H_2O_2. The presence of both water and SOA leads to the rapid
462 transformation of gaseous organic peroxides into H_2O_2. This heterogeneous process increases
463 the H_2O_2 yield by ~67%. Our results also show that water vapor affects the distribution of
464 gaseous peroxides, although it cannot change the yield of total peroxides.

465 The rapid heterogeneous transformation of organic peroxides to H_2O_2 helps to explain the
466 differences between modelled and observed levels of peroxides and OH in the forest area. In
467 the airborne GABRIEL field campaign in equatorial South America (Surinam) in October 2005
468 (Kubistin et al., 2010), two issues arose: (1) organic peroxides were overestimated while H_2O_2
469 was underestimated and (2) OH and HO_2 were also underestimated, especially when
470 concentrations of VOCs were high. These investigators suggested the occurrence of additional
471 recycling from HO_2 to OH or the contributions of additional direct OH sources. Our finding
472 that organic peroxides can transform to H_2O_2 by rapid heterogeneous reactions can address the
473 first discrepancy directly and the second indirectly. Peroxides influence OH through the
474 removal pathways:

475 $ROOH + h\nu \rightarrow RO + OH$ (R2)

476 $ROOH + OH \rightarrow RO_2 + H_2O$ (R3)

477 $H_2O_2 + h\nu \rightarrow 2OH$ (R4)

478 $H_2O_2 + OH \rightarrow H_2O + HO_2$ (R5)

479 Predominant removal paths for organic peroxides in the atmosphere are reaction with OH (95%)
480 and photolysis (4.4%) (Khan et al., 2015), while for H_2O_2, these two paths are almost equally
481 important. The OH oxidation process consumes OH while photolysis process produces OH.
482 Obviously, H_2O_2 plays a different role in the OH cycling compared with organic peroxides. One
483 molecule of organic peroxides transformed into H_2O_2 yields ~1.4 molecules of OH. Thus, the
484 rapid transformation of organic peroxides to H_2O_2 by the heterogeneous process would increase
485 OH levels. However, not all the organic peroxides could be transformed to H_2O_2 by the
486 heterogeneous process. Further studies are needed to clarify this process in the atmosphere and
487 unveil the features of the peroxides undergoing heterogeneous transformation.

488 **Acknowledgements**

We gratefully acknowledge the National Natural Science Foundation of China (grants 41275125, 21190053, 21477002) and the State Key Laboratory of Environment Simulation and Pollution Control (special fund) for financial support.

References

Aplincourt, P., and Anglada, J.: Theoretical studies on isoprene ozonolysis under tropospheric conditions. 1. Reaction of substituted carbonyl oxides with water, J. Phys. Chem.A, 107, 5798−5811, doi: 0.1021/jp026868o, 2003.

Arellanes, C., Paulson, S. E., Fine, P. M., and Sioutas, C.: Exceeding of Henry's law by hydrogen peroxide associated with urban aerosols, Environ. Sci. Technol., 40, 4859−4866, doi: 10.1021/es0513786, 2006.

Badali, K., Zhou, S., Aljawhary, D., Antiñolo, M., Chen, W., Lok, A., Mungall, E., Wong, J., Zhao, R., and Abbatt, J.: Formation of hydroxyl radicals from photolysis of secondary organic aerosol material, Atmos. Chem. Phys., 15, 7831–7840, doi: 10.5194/acp-15-7831-2015, 2015.

Banerjee, D. K., and Budke, C. C.: Spectrophotometric Determination of Traces of Peroxides in Organic Solvents, Anal. Chem., 36, 792−796, doi: 10.1021/ac60210a027, 1964.

Bateman, A. P., Nizkorodov, S. A., Laskin, J., and Laskin, A.: Photolytic processing of secondary organic aerosols dissolved in cloud droplets, Phys. Chem. Chem. Phys., 13, 12199−12212, doi: 10.1039/c1cp20526a, 2011.

Baum, E.: Chemical property estimation: Theory and Application, CRC Press, Florida, 1997.

Becker, K. H., Brockmann, K. J., and Bechara, J.: Production of hydrogen peroxide in forest air by reaction of ozone with terpenes, Nature, 346, 256−258, doi: 10.1038/346256a0, 1990.

Berndt, T., Böge, O., and Stratmann, F.: Gas-phase ozonolysis of α-pinene: gaseous products and particle formation, Atmos. Environ., 37, 3933−3945, doi: 10.1016/S1352-2310(03)00501-6, 2003.

Berndt, T., Voigtländer, J., Stratmann, F., Junninen, H., Mauldin III, R. L., Sipilä, M., Kulmala, M., and Herrmann, H.: Competing atmospheric reactions of CH_2OO with SO_2 and water vapour, Phys. Chem. Chem. Phys., 16, 19130−19136, doi: 10.1039/c4cp02345e, 2014.

Bonn, B., von Kuhlmann, R., and Lawrence, M. G.: High contribution of biogenic hydroperoxides to secondary organic aerosol formation, Geophys. Res. Lett., 31, L10108, doi: 10.1029/2003GL019172, 2004.

Camredon, M., Hamilton, J., Alam, M., Wyche, K., Carr, T., White, I., Monks, P., Rickard, A., and Bloss, W.: Distribution of gaseous and particulate organic composition during dark α-

pinene ozonolysis, Atmos. Chem. Phys., 10, 2893−2917, doi: 10.5194/acp-10-2893-2010, 2010.

Chao, W., Hsieh, J.-T., and Chang, C.-H.: Direct kinetic measurement of the reaction of the simplest Criegee intermediate with water vapor, Science, 347, 751−754, doi: 10.1126/science.1261549, 2015.

Chen, Z., Wang, H., Zhu, L., Wang, C., Jie, C., and Hua, W.: Aqueous-phase ozonolysis of methacrolein and methyl vinyl ketone: a potentially important source of atmospheric aqueous oxidants, Atmos. Chem. Phys., 8, 2255−2265, doi: 10.5194/acp-8-2255-2008, 2008.

Cocker III, D. R., Clegg, S. L., Flagan, R. C., and Seinfeld, J. H.: The effect of water on gas–particle partitioning of secondary organic aerosol. Part I: α-pinene/ozone system, Atmos. Environ., 35, 6049−6072, doi: 10.1016/S1352-2310(01)00404-6, 2001.

Crehuet, R., Anglada, J. M., and Bofill, J. M.: Tropospheric formation of hydroxymethyl hydroperoxide, formic acid, H2O2, and OH from carbonyl oxide in the presence of water vapor: a theoretical study of the reaction mechanism, Chemistry-a European Journal, 7, 2227−2235, doi: 10.1002/1521-3765(20010518)7:10<2227::AID-CHEM2227>3.3.CO;2-F, 2001.

Docherty, K. S., Wu, W., Lim, Y. B., and Ziemann, P. J.: Contributions of organic peroxides to secondary aerosol formed from reactions of monoterpenes with O_3, Environ. Sci. Technol., 39, 4049−4059, doi: 10.1021/es050228s, 2005.

Epstein, S. A., Blair, S. L., and Nizkorodov, S. A.: Direct photolysis of α-pinene ozonolysis secondary organic aerosol: effect on particle mass and peroxide content, Environ. Sci. Technol., 48, 11251−11258, doi: 10.1021/es502350u, 2014.

Farina, S. C., Adams, P. J., and Pandis, S. N.: Modeling global secondary organic aerosol formation and processing with the volatility basis set: Implications for anthropogenic secondary organic aerosol, J. Geophys. Res.-Atmos., 115, D09202, doi: 10.1029/2009JD013046, 2010.

Fu, H., Wang, X., Wu, H., Yin, Y., and Chen, J.: Heterogeneous uptake and oxidation of SO_2 on iron oxides, J. Phys. Chem.C, 111, 6077−6085, doi: 0.1021/jp070087b, 2007.

551 Gäb, S., Turner, W. V., Wolff, S., Becker, K. H., Ruppert, L., and Brockmann, K. J.: Formation
552 of alkyl and hydroxyalkyl hydroperoxides on ozonolysis in water and in air, Atmos. Environ.,
553 29, 2401−2407, doi: 10.1016/1352-2310(95)00166-V, 1995.
554 Goodman, A., Bernard, E., and Grassian, V.: Spectroscopic study of nitric acid and water
555 adsorption on oxide particles: Enhanced nitric acid uptake kinetics in the presence of
556 adsorbed water, J. Phys. Chem.A, 105, 6443−6457, doi: 10.1021/jp003722l, 2001.
557 Griffin, R. J., Cocker, D. R., Flagan, R. C., and Seinfeld, J. H.: Organic aerosol formation from
558 the oxidation of biogenic hydrocarbons, J. Geophys. Res., 104, 3555−3567, doi:
559 10.1029/1998JD100049, 1999.
560 Hellpointner, E., and Gäb, S.: Detection of methyl, hydroxymethyl and hydroxyethyl
561 hydroperoxides in air and precipitation, Nature, 337, 631−634, doi: 10.1038/337631a0, 1989.
562 Hewitt, C. N., and Kok, G. L.: Formation and occurrence of organic hydroperoxides in the
563 troposphere: laboratory and field observations, J. Atmos. Chem., 12, 181−194, doi:
564 10.1007/BF00115779, 1991.
565 Hoffmann, T., Odum, J. R., Bowman, F., Collins, D., Klockow, D., Flagan, R. C., and Seinfeld,
566 J. H.: Formation of organic aerosols from the oxidation of biogenic hydrocarbons, J. Atmos.
567 Chem., 26, 189−222, doi: 10.1023/A:1005734301837, 1997.
568 Hua, W., Chen, Z., Jie, C., Kondo, Y., Hofzumahaus, A., Takegawa, N., Chang, C., Lu, K.,
569 Miyazaki, Y., and Kita, K.: Atmospheric hydrogen peroxide and organic hydroperoxides
570 during PRIDE-PRD'06, China: their concentration, formation mechanism and contribution
571 to secondary aerosols, Atmos. chem. phys., 8, 6755−6773, doi: 10.5194/acp-8-6755-2008,
572 2008.
573 Huang, D., Chen, Z., Zhao, Y., and Liang, H.: Newly observed peroxides and the water effect
574 on the formation and removal of hydroxyalkyl hydroperoxides in the ozonolysis of isoprene,
575 Atmos. Chem. Phys., 13, 5671−5683, doi: 10.5194/acp-13-5671-2013, 2013.
576 Huang, L., Zhao, Y., Li, H., and Chen, Z.: Kinetics of heterogeneous reaction of sulfur dioxide
577 on authentic mineral dust: effects of relative humidity and hydrogen peroxide, Environ. Sci.
578 Technol., 49, 10797-10805, doi: 10.1021/acs.est.5b03930, 2015.

579 Jenkin, M.: Modelling the formation and composition of secondary organic aerosol from α-and
580 β-pinene ozonolysis using MCM v3, Atmos. Chem. Phys., 4, 1741−1757, doi: 10.5194/acp-
581 4-1741-2004, 2004.
582 Kamens, R. M., and Jaoui, M.: Modeling aerosol formation from α-pinene+ NO x in the
583 presence of natural sunlight using gas-phase kinetics and gas-particle partitioning theory,
584 Environ. Sci. Technol., 35, 1394−1405, doi: 10.1021/es001626s, 2001.
585 Khan, M., Cooke, M., Utembe, S., Xiao, P., Morris, W., Derwent, R., Archibald, A., Jenkin,
586 M., Percival, C., and Shallcross, D.: The global budgets of organic hydroperoxides for
587 present and pre-industrial scenarios, Atmos. Environ., 110, 65−74, doi:
588 10.1016/j.atmosenv.2015.03.045, 2015.
589 Kidd, C., Perraud, V., and Finlayson-Pitts, B. J.: New insights into secondary organic aerosol
590 from the ozonolysis of α-pinene from combined infrared spectroscopy and mass
591 spectrometry measurements, Phys. Chem. Chem. Phys., 16, 22706−22716, doi:
592 10.1039/c4cp03405h, 2014.
593 Kroll, J. H., Ng, N. L., Murphy, S. M., Varutbangkul, V., Flagan, R. C., and Seinfeld, J. H.:
594 Chamber studies of secondary organic aerosol growth by reactive uptake of simple carbonyl
595 compounds, J. Geophys. Res.-Atmos., 110, D23207, doi: 10.1029/2005JD006004, 2005.
596 Kubistin, D., Harder, H., Martinez, M., Rudolf, M., Sander, R., Bozem, H., Eerdekens, G.,
597 Fischer, H., Gurk, C., and Klüpfel, T.: Hydroxyl radicals in the tropical troposphere over the
598 Suriname rainforest: comparison of measurements with the box model MECCA, Atmos.
599 Chem. Phys., 10, 9705−9728, doi: 10.5194/acp-10-9705-2010, 2010.
600 Lee, M., Heikes, B. G., and O'Sullivan, D. W.: Hydrogen peroxide and organic hydroperoxide
601 in the troposphere: a review, Atmos. Environ., 34, 3475−3494, doi: 10.1016/S1352-
602 2310(99)00432-X, 2000.
603 Lewis, T. R., Blitz, M. A., Heard, D. E., and Seakins, P. W.: Direct evidence for a substantive
604 reaction between the Criegee intermediate, CH 2 OO, and the water vapour dimer, Phys.
605 Chem. Chem. Phys., 17, 4859−4863, doi: 10.1039/c4cp04750h, 2015.
606 Liggio, J., Li, S.-M., and McLaren, R.: Heterogeneous reactions of glyoxal on particulate matter:
607 Identification of acetals and sulfate esters, Environ. Sci. Technol., 39, 1532−1541, doi:
608 10.1021/es048375y, 2005.

Mertes, P., Pfaffenberger, L., Dommen, J., Kalberer, M., and Baltensperger, U.: Development of a sensitive long path absorption photometer to quantify peroxides in aerosol particles (Peroxide-LOPAP), Atmos. Meas. Tech., 5, 2339–2348, doi: 10.5194/amt-5-2339-2012, 2012.

Nguyen, T. B., Bateman, A. P., Bones, D. L., Nizkorodov, S. A., Laskin, J., and Laskin, A.: High-resolution mass spectrometry analysis of secondary organic aerosol generated by ozonolysis of isoprene, Atmos. Environ., 44, 1032–1042, doi: 10.1016/j.atmosenv.2009.12.019, 2010.

Odum, J. R., Hoffmann, T., Bowman, F., Collins, D., Flagan, R. C., and Seinfeld, J. H.: Gas/particle partitioning and secondary organic aerosol yields, Environ. Sci. Technol., 30, 2580–2585, doi: 10.1021/es950943+, 1996.

Pankow, J. F.: An absorption model of the gas/aerosol partitioning involved in the formation of secondary organic aerosol, Atmos. Environ., 28, 189–193, doi: 10.1016/1352-2310(94)90093-0, 1994.

Presto, A. A., Huff Hartz, K. E., and Donahue, N. M.: Secondary organic aerosol production from terpene ozonolysis. 2. Effect of NO x concentration, Environ. Sci. Technol., 39, 7046–7054, doi: 10.1021/es050400s, 2005.

Prince, A. P., Kleiber, P., Grassian, V., and Young, M.: Heterogeneous interactions of calcite aerosol with sulfur dioxide and sulfur dioxide–nitric acid mixtures, Phys. Chem. Chem. Phys., 9, 3432–3439, doi: 10.1039/B703296J, 2007.

Pye, H. O., and Seinfeld, J. H.: A global perspective on aerosol from low-volatility organic compounds, Atmos. Chem. Phys., 10, 4377–4401, doi: 10.5194/acp-10-4377-2010, 2010.

Reeves, C. E., and Penkett, S. A.: Measurements of peroxides and what they tell us, Chem. Rev., 103, 5199–5218, doi: 10.1021/cr0205053, 2003.

Rudich, Y., Donahue, N. M., and Mentel, T. F.: Aging of organic aerosol: Bridging the gap between laboratory and field studies, Annu. Rev. Phys. Chem., 58, 321–352, doi: 10.1146/annurev.physchem.58.032806.104432, 2007.

Ryzhkov, A. B., and Ariya, P. A.: A theoretical study of the reactions of parent and substituted Criegee intermediates with water and the water dimer, Phys. Chem. Chem. Phys., 6, 5042–5050, doi: 10.1039/B408414D, 2004.

639 Saathoff, H., Naumann, K.-H., Möhler, O., Jonsson, Å. M., Hallquist, M., Kiendler-Scharr, A.,
640 Mentel, T. F., Tillmann, R., and Schurath, U.: Temperature dependence of yields of
641 secondary organic aerosols from the ozonolysis of α-pinene and limonene, Atmos. Chem.
642 Phys., 9, 1551–1577, doi: 10.5194/acp-9-1551-2009, 2009.
643 Simonaitis, R., Olszyna, K., and Meagher, J.: Production of hydrogen peroxide and organic
644 peroxides in the gas phase reactions of ozone with natural alkenes, Geophys. Res. Lett., 18,
645 9–12, 1991.
646 Surratt, J. D., Murphy, S. M., Kroll, J. H., Ng, N. L., Hildebrandt, L., Sorooshian, A.,
647 Szmigielski, R., Vermeylen, R., Maenhaut, W., and Claeys, M.: Chemical composition of
648 secondary organic aerosol formed from the photooxidation of isoprene, J. Phys. Chem.A,
649 110, 9665–9690, doi: 10.1021/jp061734m, 2006.
650 Tobias, H. J., and Ziemann, P. J.: Thermal desorption mass spectrometric analysis of organic
651 aerosol formed from reactions of 1-tetradecene and O_3 in the presence of alcohols and
652 carboxylic acids, Environ. Sci. Technol., 34, 2105–2115, doi: 10.1021/es9907156, 2000.
653 Tobias, H. J., and Ziemann, P. J.: Kinetics of the gas-phase reactions of alcohols, aldehydes,
654 carboxylic acids, and water with the C_{13} stabilized Criegee intermediate formed from
655 ozonolysis of 1-tetradecene, J. Phys. Chem.A, 105, 6129–6135, doi: 10.1021/jp004631r,
656 2001.
657 Venkatachari, P., and Hopke, P. K.: Development and laboratory testing of an automated
658 monitor for the measurement of atmospheric particle-bound reactive oxygen species (ROS),
659 Aerosol Sci. Technol., 42, 629–635, doi: 10.1039/b804357d, 2008.
660 Vereecken, L., Harder, H., and Novelli, A.: The reactions of Criegee intermediates with alkenes,
661 ozone, and carbonyl oxides, Phys. Chem. Chem. Phys., 16, 4039–4049, doi:
662 10.1039/c3cp54514h, 2014.
663 Wang, Y., Kim, H., and Paulson, S. E.: Hydrogen peroxide generation from α-and β-pinene and
664 toluene secondary organic aerosols, Atmos. Environ., 45, 3149–3156, doi:
665 10.1016/j.atmosenv.2011.02.060, 2011.
666 Yu, J., Cocker III, D. R., Griffin, R. J., Flagan, R. C., and Seinfeld, J. H.: Gas-phase ozone
667 oxidation of monoterpenes: Gaseous and particulate products, J. Atmos. Chem., 34, 207–258,
668 doi: 10.1023/A:1006254930583, 1999.

669 Zhang, X., Chen, Z., Wang, H., He, S., and Huang, D.: An important pathway for ozonolysis
670 of alpha-pinene and beta-pinene in aqueous phase and its atmospheric implications, Atmos.
671 Environ., 43, 4465−4471, doi: 10.1016/j.atmosenv.2009.06.028, 2009.
672 Zhao, Y., Chen, Z., and Zhao, J.: Heterogeneous reactions of methacrolein and methyl vinyl
673 ketone on α-Al_2O_3 particles, Environ. Sci. Technol., 44, 2035−2041, doi: 10.1021/es9037275,
674 2010.
675 Zhao, Y., Chen, Z., Shen, X., and Zhang, X.: Kinetics and mechanisms of heterogeneous
676 reaction of gaseous hydrogen peroxide on mineral oxide particles, Environ. Sci. Technol.,
677 45, 3317−3324, doi: 10.1021/es104107c, 2011.
678 Zhao, Y., Huang, D., Huang, L., and Chen, Z.: Hydrogen peroxide enhances the oxidation of
679 oxygenated volatile organic compounds on mineral dust particles: a case study of
680 methacrolein, Environ. Sci. Technol., 48, 10614−10623, doi: 10.1021/es5023416, 2014.
681 Zhou, X., and Lee, Y. N.: Aqueous solubility and reaction kinetics of hydroxymethyl
682 hydroperoxide, J. Phys. Chem., 96, 265−272, doi: 10.1021/j100180a051, 1992.
683 Ziemann, P. J.: Aerosol products, mechanisms, and kinetics of heterogeneous reactions of
684 ozone with oleic acid in pure and mixed particles, Faraday Discuss., 130, 469−490, doi:
685 10.1039/b417502f, 2005.
686
687
688

689 **Table 1.** Peroxide content in the gas phase and particle phase of α-pinene ozonolysis as affected by the OH
690 radical scavenger cyclohexane[a].

OH scavenger	None		Cyclohexane	
RH	<0.5%	60%	<0.5%	60%
		Gas phase		
Y^{b}_{H2O2}	0.048 ±0.012	0.16 ±0.01	0.048 ±0.010	0.14 ±0.02
Y^{b}_{HMHP}	0.0030 ±0.0003	0.0062 ±0.0005	0.0024 ±0.0005	0.0037 ±0.0006
Y^{b}_{PFA}	0.0057 ±0.0020	0.012 ±0.002	0.0020 ±0.0003	0.005 ±0.001
Y^{b}_{PAA}	0.0067 ±0.0006	0.009 ±0.001	0.0022 ±0.0002	0.0024 ±0.0001
Y^{b}_{TPO}	0.18 ±0.01	0.20 ±0.01	0.27 ±0.02	0.25 ±0.02
H_2O_2(g)/TPO(g) (ppbv ppbv^{-1})	0.26 ±0.02	0.78 ±0.04	0.18 ±0.02	0.50 ±0.04
		Particle phase		
Y^{c}_{SOA}	0.41 ±0.01	0.39 ±0.02	0.28 ±0.02	0.27 ±0.01
F^{d}_{H2O2} (ng μg^{-1})	5.09 ±0.99	2.67 ±0.17	1.61 ±0.11	1.41 ±0.21
F^{d}_{PFA} (ng μg^{-1})	0.35 ±0.06	0.27 ±0.02	0.14 ±0.01	0.16 ±0.04
F^{d}_{PAA} (ng μg^{-1})	0.11 ±0.04	0	0.09 ±0.01	0
F^{d}_{TPO} (μg μg^{-1})	0.23 ±0.01	0.25 ±0.01	0.16 ±0.01	0.20 ±0.01
H_2O_2(p)/TPO(p) (μM μM^{-1})	0.20 ±0.03	0.10 ±0.01	0.09 ±0.01	0.06 ±0.01
TPO(p)/TPO(g+p)[e]	0.19 ±0.02	0.18 ±0.03	0.07 ±0.01	0.09 ±0.01

691 [a] ~275 ppbv α-pinene, ~1300 ppmv cyclohexane and ~42 ppmv O_3 were used in these experiments. The data
692 represent the mean ± s.d. of 3 observations.
693 [b] molar yield of peroxides
694 [c] mass yield of SOA
695 [d] contribution of peroxides to SOA mass
696 [e] fraction of particulate TPO in gaseous and particulate TPO
697

Table 2. Comparison of observed and theoretical gas-particle partitioning coefficients (K_p) of PFA, PAA and TPO at different scenarios (298K).

	K_p (observed) $(m^3\ \mu g^{-1})$[a]				K_p (theoretical) $(m^3\ \mu g^{-1})$
	Sc1	Sc2	Sc3	Sc4	
PFA	8.06×10^{-5}	2.95×10^{-5}	9.19×10^{-5}	4.20×10^{-5}	2×10^{-9}
PAA	1.76×10^{-5}	0	4.38×10^{-5}	0	4×10^{-9}
TPO	3.47×10^{-4}	3.39×10^{-4}	1.61×10^{-4}	2.17×10^{-4}	–

[a] The four scenarios represent four reaction conditions: Sc1 (<0.5% RH, no OH scavenger), Sc2 (60% RH, no OH scavenger), Sc3 (<0.5% RH, with cyclohexane) and Sc4 (60% RH, with cyclohexane). Cyclohexane used here was ~1300 ppmv.

Table 3. Hydrogen peroxide in the coil collector at different scenarios in the two-stage experiments.

Scenarios	Filter position[a]	Water vapor[b]	H_2O_2	Species in second reactor
1d	Second reactor	No	100 ±1%	Gaseous products, SOA
1w	Second reactor	Yes	165 ±6%	Gaseous products, SOA, water vapor
2d	First reactor	No	103 ±6%	Gaseous products
2w	First reactor	Yes	87 ±7%	Gaseous products, water vapor
3d	No filter	No	164 ±9%	Gaseous products, SOA[c]
3w	No filter	Yes	172 ±5%	Gaseous products, SOA, water vapor

[a] The filters were placed at the outlet of the first reactor or second reactor.

[b] Water vapor was induced into the second reactor.

[c] Although gaseous products and SOA did not contact water vapor in the second reactor, they were in contact with the condensed water in the coil collector.

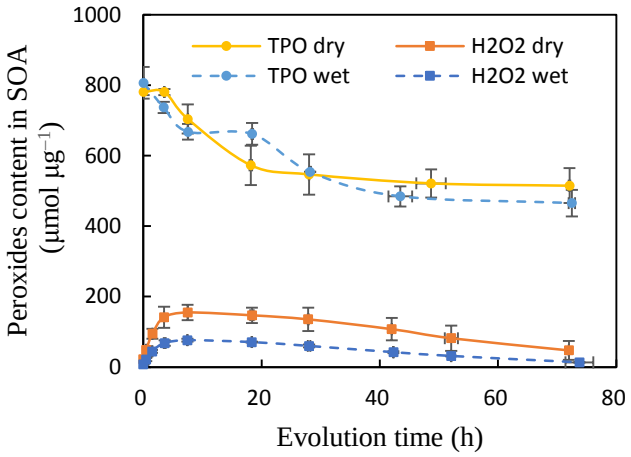

Figure 1. Evolution of total peroxides and H_2O_2 contents in SOA produced under dry (<0.5% RH) and wet (60% RH) conditions at 298K. Circles and diamonds represent total peroxides and H_2O_2 contents in SOA, respectively; and solid lines and dash lines represent that obtained under dry and wet conditions, respectively. The data represent the mean ± s.d. of 3 observations.

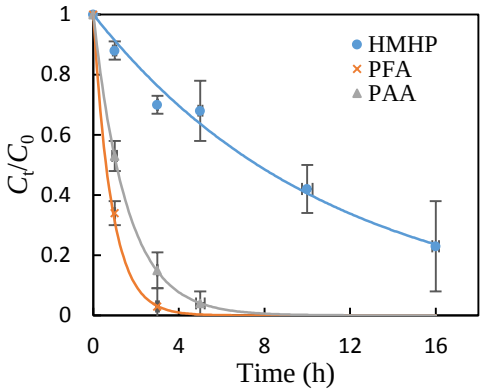

Figure 2. Decomposition/hydrolysis of organic peroxides in the aqueous phase. C_t/C_0 is the ratio of peroxides concentration at time = t h to peroxides concentration at time = 0 h. Lines are exponential fits for HMHP, PFA and PAA. The decay rate constants of HMHP, PFA and PAA are 0.09, 1.06 and 0.64 h^{-1}, respectively. The data represent the mean ± s.d. of 3 observations.